



## Original Articles

SHC4 orchestrates  $\beta$ -catenin pathway-mediated metastasis in triple-negative breast cancer by promoting Src kinase autophosphorylation

Wenjing Zhong<sup>a,b,1</sup>, Yunting Jian<sup>c,1</sup>, Chao Zhang<sup>a,b,1</sup>, Yue Li<sup>a</sup>, Zhongyu Yuan<sup>f</sup>, Zhenchong Xiong<sup>a,b</sup>, Weiling Huang<sup>a,b</sup>, Ying Ouyang<sup>a</sup>, Xiangfu Chen<sup>a</sup>, Libing Song<sup>a,\*\*</sup>, Pian Liu<sup>d,e,\*\*\*</sup>, Xi Wang<sup>a,b,\*</sup>

<sup>a</sup> Department of Experimental Research, State Key Laboratory of Oncology in South China, Collaborative Innovation Center for Cancer Medicine, Sun Yat-sen University Cancer Center, Guangzhou, 510060, China

<sup>b</sup> Department of Breast Surgery, State Key Laboratory of Oncology in Southern China, Collaborative Innovation Center for Cancer Medicine, Sun Yat-sen University Cancer Center, Sun Yat-sen University, Guangzhou, 510060, China

<sup>c</sup> Department of Pathology, Key Laboratory of Reproduction and Genetics of Guangdong Higher Education Institutes, Key Laboratory for Major Obstetric Diseases of Guangdong Province, The Third Affiliated Hospital of Guangzhou Medical University, Guangzhou, 510150, China

<sup>d</sup> Cancer Center, Union Hospital, Tongji Medical College, Huazhong University of Science and Technology, Wuhan, 430022, China

<sup>e</sup> Institute of Radiation Oncology, Union Hospital, Tongji Medical College, Huazhong University of Science and Technology, Wuhan, 430022, China

<sup>f</sup> Department of Medical Oncology, The State Key Laboratory of Oncology in South China, Collaborative Innovation Center for Cancer Medicine, Sun Yat-sen University Cancer Center, Sun Yat-sen University, Guangzhou, 510060, China

## ARTICLE INFO

## ABSTRACT

## Keywords:

Triple-negative breast cancer  
Tumor metastasis  
SHC4  
Src kinase

Triple-negative breast cancer (TNBC) is highly aggressive and metastatic, and has the poorest prognosis among all breast cancer subtypes. Activated  $\beta$ -catenin is enriched in TNBC and involved in Wnt signaling-independent metastasis. However, the underlying mechanisms of  $\beta$ -catenin activation in TNBC remain unknown. Here, we found that SHC4 was upregulated in TNBC and high SHC4 expression was significantly correlated with poor outcomes. Overexpression of SHC4 promoted TNBC aggressiveness *in vitro* and facilitated TNBC metastasis *in vivo*. Mechanistically, SHC4 interacted with Src and maintained its autophosphorylated activation, which activated  $\beta$ -catenin independent of Wnt signaling, and finally upregulated the transcription and expression of its downstream genes *CD44* and *MMP7*. Furthermore, we determined that the PxPPxPxxxPxP sequence on CH2 domain of SHC4 was critical for SHC4-Src binding and Src kinase activation. Overall, our results revealed the mechanism of  $\beta$ -catenin activation independent of Wnt signaling in TNBC, which was driven by SHC4-induced Src autophosphorylation, suggesting that SHC4 might be a potential prognostic marker and therapeutic target in TNBC.

## 1. Background

Triple-negative breast cancer (TNBC) is a more aggressive disease with a higher rate of relapse and distant metastasis than other breast cancer subtypes [1,2], and lacks clinicopathological expression of estrogen receptor (ER), progesterone receptor (PR), and human epidermal growth factor receptor 2 (HER2). Patients with TNBC generally have poor outcomes not only because they cannot benefit from endocrine therapy or anti-HER2 therapy, but also because of the intrinsic TNBC

features, for example, malignant invasion and migration [3,4]. However, the underlying mechanisms that drive TNBC aggressiveness are not fully understood, and it is imperative to explore new therapeutic targets against TNBC.

$\beta$ -catenin is known as a key protein that regulates downstream genes following Wnt pathway activation. Recently, it is noticed that  $\beta$ -catenin can also be activated by other signaling pathways that do not rely on Wnt. The dynamic interaction of  $\beta$ -catenin with cadherin allows Wnt-independent  $\beta$ -catenin activation. Phosphorylation by the tyrosine

\* Corresponding author. Department of Breast Surgery, Sun Yat-sen University Cancer Center, Sun Yat-sen University, Guangzhou, 510060, China.

\*\* Corresponding author. Department of Experimental Research, Sun Yat-sen University Cancer Center, Guangzhou 510060, China.

\*\*\* Corresponding author. Cancer Center, Union Hospital, Tongji Medical College, Huazhong University of Science and Technology, Wuhan 430022, China.

E-mail addresses: [songlb@sysucc.org.cn](mailto:songlb@sysucc.org.cn) (L. Song), [liupianamazing@126.com](mailto:liupianamazing@126.com) (P. Liu), [wangxi@sysucc.org.cn](mailto:wangxi@sysucc.org.cn) (X. Wang).

<sup>1</sup> These authors contributed equally to this work.

<https://doi.org/10.1016/j.canlet.2023.216516>

Received 7 September 2023; Received in revised form 10 November 2023; Accepted 23 November 2023

Available online 3 December 2023

0304-3835/© 2023 Elsevier B.V. All rights reserved.

kinases epidermal growth factor receptor (EGFR) or Src disrupts  $\beta$ -catenin binding to E-cadherin and increases cytoplasmic  $\beta$ -catenin levels [5]. The activation of tyrosine kinases increases  $\beta$ -catenin signaling in the nucleus and upregulates TCF-mediated gene transcription [6], to promote cell migration, and cancer progression [7]. Nuclear and cytosolic accumulation of  $\beta$ -catenin is enriched in basal-like breast cancer (BLBC, a molecular subtype with 80 % overlap with TNBC) and predictive of worse overall survival (OS) [8,9]. However, the underlying mechanisms of  $\beta$ -catenin activation in TNBC remain unknown. In this process, adaptor proteins are important in kinase activation, signal transduction, and downstream protein recruitment.

SHC4 is a member of the SHC family and is characterized by a phosphotyrosine binding (PTB) domain and Src homology 2 (SH2) domain, which both bind to phosphorylated tyrosine residues on cell surface receptors and other signaling proteins. SHC family proteins contain the proline- and glycine-rich domains termed collagen homology 1 (CH1) and CH2 domains, which act as docking sites for certain proteins [10,11]. Abnormal SHC4 expression promotes cell migration and invasion in melanoma [12], glioma [13], and hepatocellular carcinoma [14]. Notably, Maind et al. used a bioclustering algorithm and gene co-expression network to determine that *SHC4* and other specific key genes from BLBC were important in cancer progression [15]. However, the functions and regulatory mechanisms of SHC4 in TNBC remain unknown.

In the present study, we determined that SHC4 interacts with and promotes Src autophosphorylation to activate  $\beta$ -catenin independent of Wnt signaling in TNBC.  $\beta$ -catenin shed from E-cadherin via phosphorylation at Y654 and is further phosphorylated at S675 in the cytoplasm, which promote its translocation into the nucleus and upregulate the transcription of the invasion- and metastasis-related genes matrix metalloproteinase (MMP)7 and CD44. Therefore, our findings uncover a novel mechanism of SHC4/Src/ $\beta$ -catenin activation and suggest that SHC4 might be a promising prognostic marker and a therapeutic target in patients with TNBC.

## 2. Methods

### 2.1. Study cohort and patient specimens

We retrospectively identified patients with stage I-III breast cancer who underwent surgery between 2008 and 2012 at the Sun Yat-sen University Cancer Center. The breast cancer diagnosis was based on pathological examination. The cases were staged according to the criteria of the eighth edition of the American Joint Committee on Cancer tumor-node-metastasis (TNM) classification. All patients received a standardized follow-up protocol, and the median follow-up duration was 70 months (range: 2–164 months). Eventually, 256 non-TNBC cases and 112 TNBC cases were enrolled. Detailed clinicopathological and survival data were collected (Supplementary Table 1). The Sun Yat-sen University Cancer Center ethics committee approved the study.

### 2.2. Cell lines and cell culture

MCF-10A, MCF-7, ZR-75-1, SKBR-3, MDA-MB-231, BT-549, Hs578t, and 4T1 cells were from American Type Culture Collection and SUM159PT cells were from Asterand Bioscience. All cells were cultured in Dulbecco's modified Eagle's medium supplemented with 10% FBS, 100 U/ml penicillin, and 100  $\mu$ g/ml streptomycin at 37 °C in a humidified incubator containing 5% CO<sub>2</sub>. The cell lines included in our study were profiled by short tandem repeat testing at the beginning of our experiments. The Supplementary Data-Materials and methods section describes the other experiments conducted in this study.

### 2.3. Immunohistochemical (IHC) staining

SHC4 in 368 paraffin-embedded breast cancer specimens was

determined with IHC staining using an anti-SHC4 antibody (12641-1-AP, Proteintech). And IHC staining was performed consecutive paraffin sections in 112 TNBC patients using anti-phospho-Src (Tyr419) antibody (TA3162, Abmart) and anti- $\beta$ -catenin antibody (#8480, CST). Sections (4- $\mu$ m thick) from the paraffin-embedded specimens were baked at 65 °C for 1.5 h, deparaffinized with xylene and rehydrated, submerged in EDTA antigenic retrieval buffer, and microwaved for antigenic retrieval. The samples were treated with 3% hydrogen peroxide in methanol to quench the endogenous peroxidase activity, incubated with 1% bovine serum albumin (BSA) to block nonspecific binding, and subsequently incubated with primary antibodies overnight at 4 °C. After washing, the tissue sections were treated with biotinylated secondary antibody, then incubated with streptavidin-horseradish peroxidase complex (Zsbio). Finally, the peroxidase reaction was developed with diaminobenzidine (Zsbio) and counterstained with 10% Mayer's hematoxylin, dehydrated, and mounted with Crystal Mount. Two independent pathologists blinded to the clinical outcomes evaluated and scored the staining results. On the one hand, the SHC4 and Src (pY419) staining were graded as follows: strong, +3; moderate, +2; weak, +1; and negative, 0. Specimens that scored +3 and +2 were defined as high expression, while those that scored +1 or 0 were low expression. Accordingly, the samples were segregated into two groups (high and low expression) for further analysis. On the other hand, specimens with > 10% nuclear  $\beta$ -catenin expression were defined as nuclear  $\beta$ -catenin-positive, and specimens with ≤ 10% nuclear  $\beta$ -catenin expression were nuclear  $\beta$ -catenin-negative [16].

### 2.4. TOP/FOP-flash activity assays

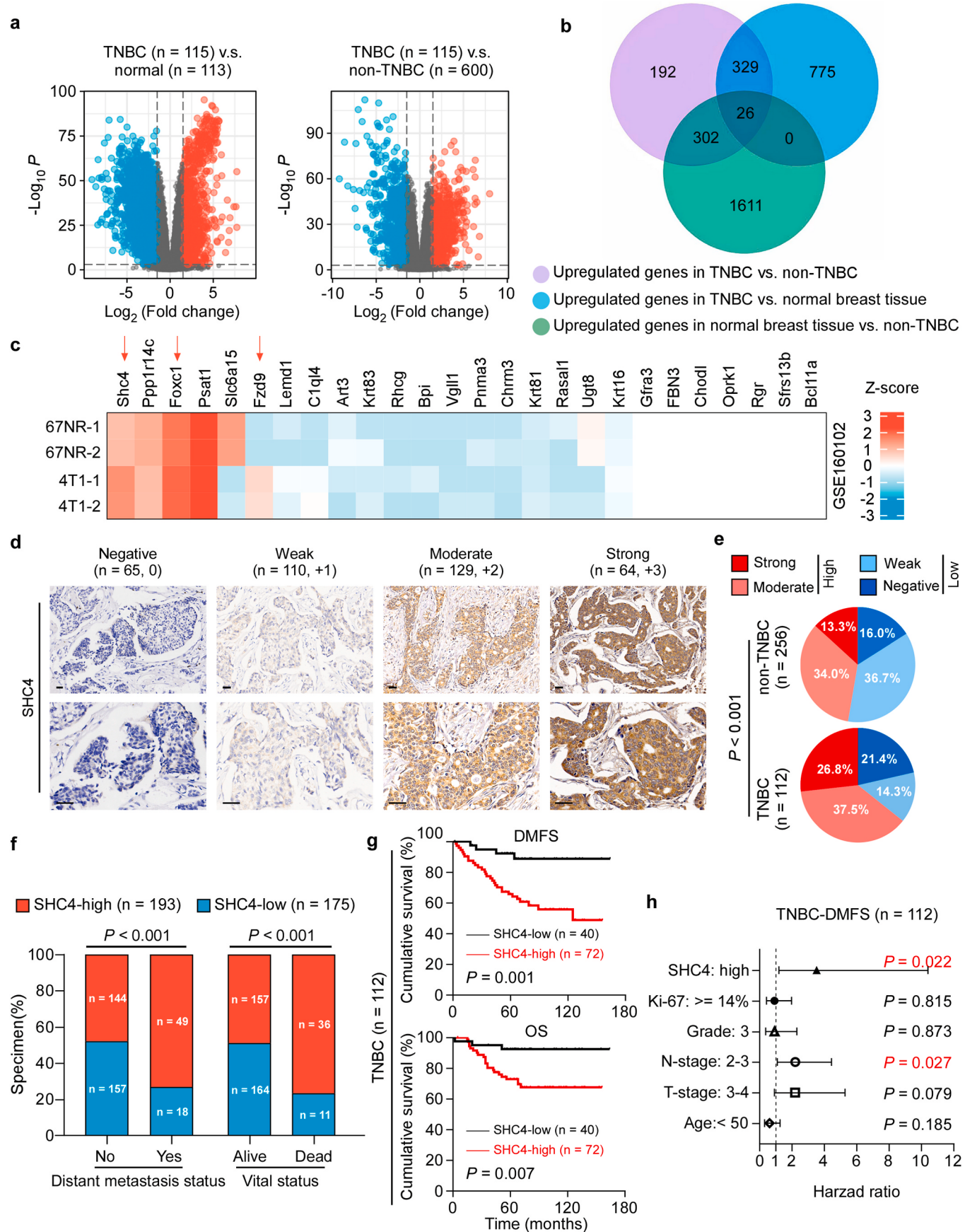
The recombinant protein Wnt3A and small-molecular inhibitor of Wnt signaling Wnt-C59 were from R&D Systems. Before cytokine treatment, the cells were changed to culture with 1% FBS medium for 1 h. Then, Wnt3A was added to a final concentration of 50 ng/ml. For the Wnt-C59 treatment, the cells were pre-treated with 100 nM Wnt-C59 for 48 h before the experiment. The wild-type (TOP) and mutant (FOP) LEF/TCF reporters were cloned into pGL3 luciferase constructs (Promega). Cells (20,000) were seeded in triplicate in 48-well plates and allowed to settle for 24 h. The cells were transfected with 100 ng TOP- or FOP-Flash plus 1 ng pRLTK *Renilla* plasmid (Promega) using the Lipofectamine 3000 reagent according to the manufacturer's recommendation. Luciferase and *Renilla* signals were measured 24 h after transfection using a Dual Luciferase Reporter Assay Kit (Promega) according to the manufacturer's protocol. The results were calculated as the ratio of specific TOP-Flash over non-specific FOP-Flash relative *Renilla* luciferase units (RLU).

### 2.5. Co-immunoprecipitation (Co-IP)

Cell lysates were prepared using lysis buffer (150 mM NaCl, 10 mM HEPES, pH 7.4, 1% NP-40), then incubated with anti-SHC4 (12641-1-AP, Proteintech) or anti-Src (#2109, Cell Signaling Technology) antibodies, and protein G-conjugated agarose or Flag or HA affinity agarose (Sigma-Aldrich) at 4 °C overnight. Beads containing affinity-bound proteins were washed six times with IP wash buffer (150 mM NaCl, 10 mM HEPES, pH 7.4, 0.1% NP-40), followed by elution with 1 M glycine (pH 3.0). The eluates were then mixed with sample buffer, denatured, and used for western blot analysis. The target proteins were blotted with primary antibodies derived from biological sources different from those used in the IP to avoid high background. Proteins that potentially interacted with SHC4 were detected by SDS-PAGE and silver staining, then identified by mass spectrometry (MS).

### 2.6. Xenograft tumor models

The Sun Yat-sen University Institutional Animal Care and Use Committee approved all animal experiments (L102022022030I).



(caption on next page)

**Fig. 1. SHC4 is substantially upregulated in TNBC and high SHC4 expression indicates poor prognosis in patients with TNBC.** (a) Volcano plots showing gene expression in TCGA breast cancer dataset comparing TNBC tissues ( $n = 115$ ) with normal tissues ( $n = 113$ ) (left) and TNBC tissues ( $n = 115$ ) with non-TNBC tissues ( $n = 600$ ) (right). Blue dots: Downregulated genes; red dots: upregulated genes.  $-\log_{10}P > 3$  was considered statistically significant. (b) Venn diagram of upregulated genes in TNBC compared with non-TNBC samples, TNBC compared to normal samples, and normal tissues compared to non-TNBC tissues. (c) Heat map of GSE160102 depicts the mean centered z-score of the 26 genes upregulated in TNBC across 67NR cells and 4T1 cells. Arrow represents  $\log_2$  (fold change + 1) > 1 and  $\log_2$  (mRNA expression of 4T1 cells + 1) > 0. (d) Representative images of SHC4 IHC staining in 112 TNBC and 256 non-TNBC specimens. Scale bar: 50  $\mu$ m. (e) Comparison of the distribution of SHC4 staining in TNBC and non-TNBC patient specimens via the  $\chi^2$  test. (f) Distribution and correlation between SHC4 staining and the tumor metastasis and patient survival statuses via the  $\chi^2$  test. (g) DMFS (top) and OS (bottom) curves of 112 patients with TNBC stratified by low and high SHC4 expression (log-rank test). (h) Multivariate Cox regression analysis evaluation of the significance of the association between SHC4 expression and DMFS in the presence of other clinicopathological characteristics in the 112 patients.

Briefly, 4-5-week-old female BALB/c-*nu* mice (weight: 18–20 g) were provided by the Guangdong Medical Laboratory Animal Center. The mice were raised in a specific pathogen-free-levelled barrier system in the Sun Yat-sen University Laboratory Animal Center. To generate the orthotopic xenograft model and spontaneous metastasis models, 4T1-luci cells ( $2 \times 10^5$ ,  $n = 6$  per group) were orthotopically injected into the mammary fat pads of the mice. Tumor volumes were determined every week, and metastases were detected using the Xenogen IVIS Spectrum Imaging System (Caliper Life Sciences) by blocking the orthotopic tumor signals. After 9 weeks, the mice were killed and their tumors and lungs were removed, extraction for protein precipitation or fixed in formalin, and embedded in paraffin.

For the lung colonization model, the mice were randomly divided into groups ( $n = 6$  per group) and treated by intravenous injection with  $5 \times 10^5$  MDA-MB-231-luci cells ( $n = 6$  per group). The lung metastasis burden of the mice was monitored weekly using bioluminescent imaging (BLI). The mice were killed 8 weeks after inoculation and the lungs were removed, fixed in formalin, and embedded in paraffin.

## 2.7. Statistical analysis

Statistical analyses were performed using SPSS 26.0. Data are reported as the means  $\pm$  S.D.. Continuous variables with the normal distribution were compared by a two-tailed Student's t-test. Qualitative variables and non-normally distributed continuous variables were analyzed by the Chi-square test. Kaplan-Meier analysis was used for univariate survival analysis and the log-rank test was applied to compare different survival curves. For the multivariate analysis, Cox regression analysis was applied. A  $P$ -value lower than 0.05 at two sides was deemed statistically significant.

## Availability of data and materials

The sequence data generated in this study are publicly available in GEO at GSE160102 and in TCGA breast cancer dataset at [<https://porta1.gdc.cancer.gov/>].

## 3. Results

### 3.1. SHC4 is substantially upregulated in TNBC and high SHC4 expression indicates poor prognosis in patients with TNBC

The identification of genes specifically dysregulated in TNBC is expected to provide potential molecular therapy targets. Therefore, we first analyzed the Cancer Genome Atlas (TCGA) breast cancer dataset and identified 26 genes that were significantly increased in TNBC by at least 2-fold compared to that in normal and non-TNBC tissues (Fig. 1a and b). To search for potential metastasis-related genes in these 26 specifically upregulated genes, we investigated their mRNA expression in low- and high-metastatic potential murine mammary tumor cells, 67NR and 4T1, respectively, through the Gene Expression Omnibus (GEO) database (GSE160102). The results demonstrated that *SHC4*, *FOXC1*, and *FZD9* expression was significantly increased in 4T1 cells compared to that in 67NR cells (Fig. 1c). Furthermore, the Kaplan-Meier plotter (<http://kmplot.com/analysis>) survival curves of the three genes

demonstrated that only patients with high *SHC4* expression had significantly poor overall survival (OS) and distant metastasis-free survival (DMFS) among the BLBC patients (Supplementary Figs. 1a–c). Therefore, we explored the potential roles of *SHC4* in TNBC. Real-time PCR and western blotting revealed that *SHC4* was significantly upregulated in TNBC cell lines and tumor tissues as compared to that in normal breast and non-TNBC tissues (Supplementary Figs. 1d and 1e).

Next, we assessed *SHC4* expression in the 368 breast cancer specimens (256 non-TNBC and 112 TNBC) (Fig. 1d and Supplementary Table 1). *SHC4* IHC scoring revealed that patients with TNBC had significantly increased *SHC4* expression (Fig. 1e). Correlation analysis demonstrated that high *SHC4* expression was significantly associated with distant metastasis and dead status (Fig. 1f). Importantly, TNBC patients with high *SHC4* expression experienced poor DMFS and OS (Kaplan-Meier survival curves and log-rank test;  $P = 0.001$ ;  $P = 0.007$ , respectively; Fig. 1g). High *SHC4* expression and advanced N stage were identified as independent prognostic factors for five-year DMFS in TNBC by multivariate regression analysis (Fig. 1h and Supplementary Table 2). Collectively, these results revealed that a robust increase in *SHC4* might be significant in breast cancer progression, specifically in TNBC.

### 3.2. *SHC4* promotes TNBC aggressiveness *in vitro*

We selected the MDA-MB-231 and SUM159PT cell lines for the gain-and loss-of-function assays, as these two cell lines had medium *SHC4* expression levels and were suitable for *SHC4* overexpression or knock-down modifications. *SHC4* was exogenously transduced or endogenously silenced in the above cell lines (Supplementary Fig. 2a), and *SHC4* overexpression obviously enhanced cell colony formation, whereas knocking down *SHC4* suppressed it (Supplementary Fig. 2b). We conducted soft agar colony formation, wound healing and transwell matrix invasion assays. The results revealed that *SHC4* overexpression promoted cell anchorage-independent TNBC cell growth, migration, and invasion capacity. Contrastingly, depleting *SHC4* exerted opposite effects (Fig. 2a–c). Notably, the 3-dimensional (3D) spheroid invasion assay demonstrated that *SHC4*-overexpressing cells displayed an invasive phenotype and satellite projections that bridged multiple cell colonies. However, silencing *SHC4* resulted in reduced invasive capacity and the formation of smaller spheroids on the matrigel (Fig. 2d). The above results showed that *SHC4* played an important role in TNBC aggression.

### 3.3. *SHC4* facilitates TNBC growth and metastasis *in vivo*

We assessed the effects of *SHC4* on TNBC progression with *in vivo* tumor models. According to the results from orthotopic xenograft model and spontaneous metastasis model, compared with the control groups, tumor growth was remarkably accelerated in the *SHC4*-overexpressing group and was suppressed in the *SHC4*-silenced group (Fig. 3a). In order to compare lung metastases in each group with similar orthotopic tumor burden, we chose to show different days of mice luminescence pictures. Moreover, even with similar orthotopic tumor burden, *SHC4* overexpression markedly increased the number of lung metastatic nodules, while silencing *SHC4* reversed this process (Fig. 3b–d). Subsequently, we found that the levels of the metastatic markers MMP-7 and

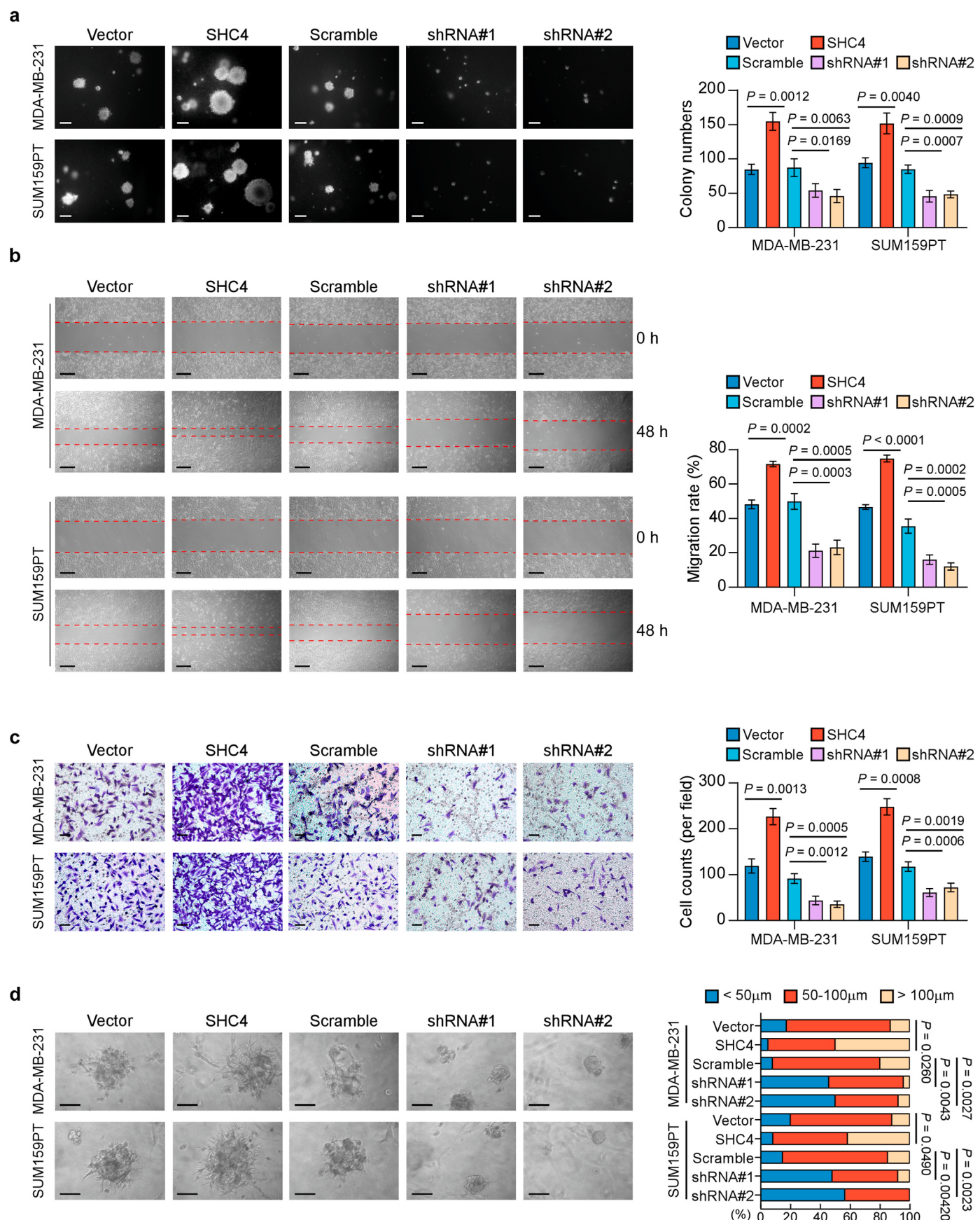
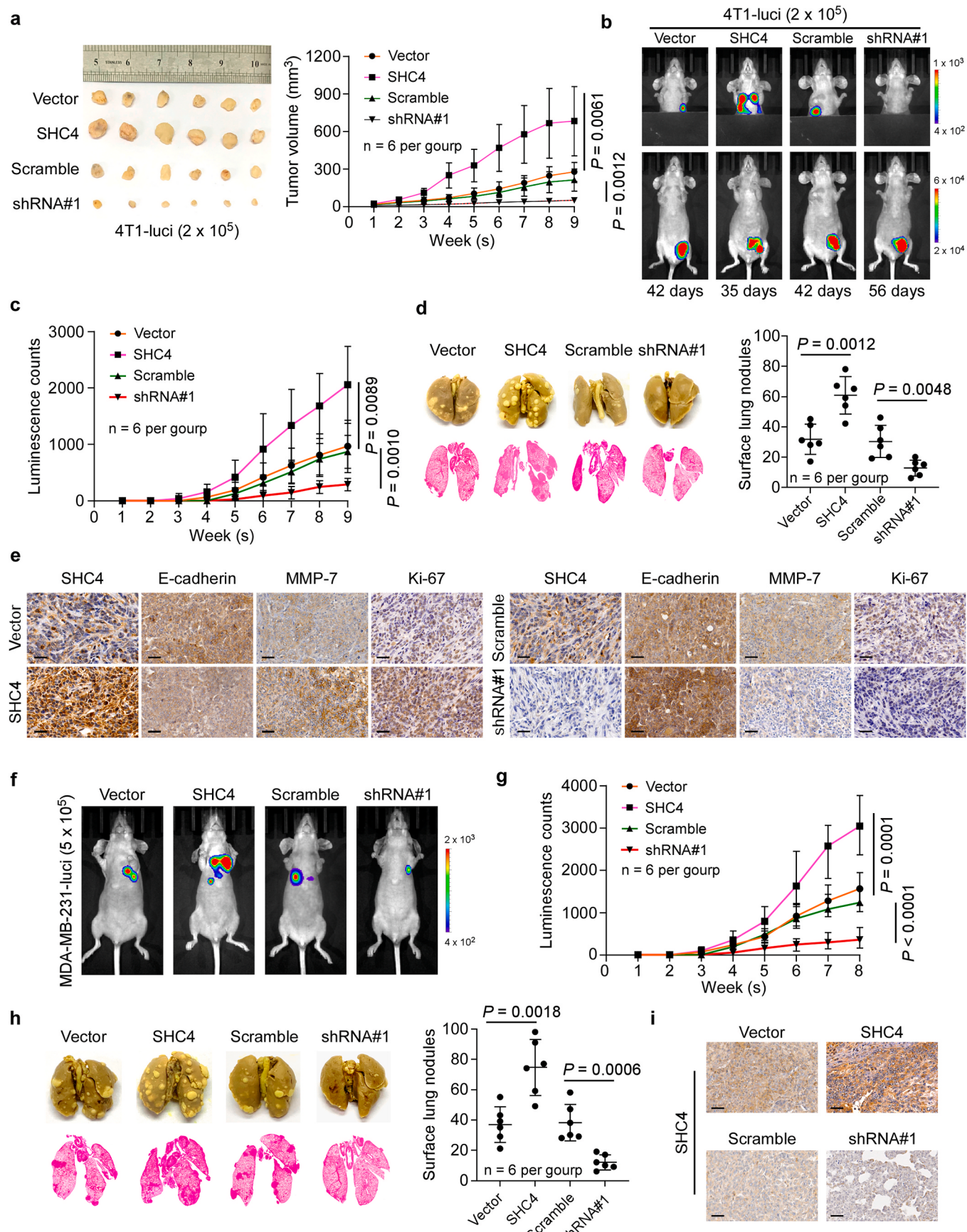


**Fig. 2. SHC4 promotes TNBC aggressiveness *in vitro*.** (a-d) Representative images (left) and quantification (right) of anchorage-independent growth colony formation (a), wound healing assay (b), transwell migration assay (c), and 3D spheroid culture assay (d). Scale bar: 50  $\mu$ m. Two-tailed Student's t-test and  $\chi^2$  test were used. Data represent the means  $\pm$  S.D. of three independent experiments.



(caption on next page)

**Fig. 3. SHC4 facilitates TNBC growth and metastasis *in vivo*.** (a) Orthotopic xenograft model and spontaneous metastasis model: SHC4-overexpressing, SHC4-silenced, and control 4T1-luci cells were injected into the mammary fat pads of nude mice. Photographs of the xenograft tumors isolated from nude mice (left) and the tumor volumes in each group (right) are shown. (b) Representative BLI of lung metastasis was photographed after blocking the orthotopic tumor signals. (c) Lung metastasis burden of each group was monitored weekly using BLI. (d) Representative bright-field imaging and H&E confirmation of lung metastases (left). The number of visible surface lesions (right) are reported as the mean  $\pm$  S.D.. (e) IHC staining of SHC4, E-cadherin, MMP-7, and Ki-67 in 4T1-luci tumors. (f) Lung colonization model of SHC4-overexpressing, SHC4-silenced, and control MDA-MB-231-luci cells. Representative BLI of lung metastasis is shown. (g) Lung metastatic burden was monitored weekly using BLI. (h) Representative bright-field imaging and H&E confirmation of lung metastases (left). The number of visible surface lesions (right) are reported as the mean  $\pm$  S.D.. (i) IHC staining of SHC4 in MDA-MB-231-luci tumors. Scale bar: 50  $\mu$ m. Two-tailed Student's t-test and log-rank test were used.

Ki-67 were increased and E-cadherin was decreased in the orthotopic 4T1-luci-SHC4 tumors, while silencing SHC4 yielded opposite results (Fig. 3e and Supplementary Fig. 3a).

The effects of SHC4 on TNBC metastasis were determined in the lung colonization model. MDA-MB-231-luci cell lines were injected into the tail veins of the mice and the metastatic burdens were monitored weekly according to BLI. Similarly, upregulating SHC4 increased the lung metastatic burdens, while silencing SHC4 significantly reduced the lung metastatic lesions (Fig. 3f-i).

### 3.4. SHC4 activates $\beta$ -catenin in a Wnt-independent manner

To determine the molecular mechanism underlying the SHC4-induced effects on TNBC aggressive capacity, we first analyzed the gene set enrichment analysis (GSEA) of TCGA breast cancer sample data to identify SHC4-related oncogenic signals. The GSEA identified significant enrichment of a  $\beta$ -catenin-upregulated gene signature in high-SHC4 samples (Fig. 4a). Intriguingly, SHC4 overexpression increased  $\beta$ -catenin activity in the absence of Wnt3a signaling stimulation (Fig. 4b). Furthermore, SHC4 overexpression increased the mRNA expression of the typical  $\beta$ -catenin downstream genes *MMP7* and *CD44* (Fig. 4c and d), which are crucial breast cancer aggressiveness and metastasis markers. Next, we investigated whether SHC4 could activate  $\beta$ -catenin in a Wnt-independent manner. Wnt-C59 is small molecular inhibitor of Wnt signaling that suppresses porcupine O-acetyltransferase (PORCN), which is required for Wnt palmitoylation and secretion [17]. Wnt-C59 inhibited Wnt3A-mediated activation of Wnt signaling in both MDA-MB-231 and SUM159PT cells (Fig. 4e). We then used Wnt-C59 to abolish Wnt ligand secretion in MDA-MB-231-vector or -SHC4 cells, and the result showed that SHC4-overexpressing cells could still activate  $\beta$ -catenin signaling in a Wnt-independent manner (Fig. 4f). Furthermore, the Wnt-C59 treatment failed to block the overexpressed SHC4 from promoting cell migration and invasion (Fig. 4g-i).

### 3.5. SHC4 binds and activates Src kinase by promoting its autophosphorylation at Y419

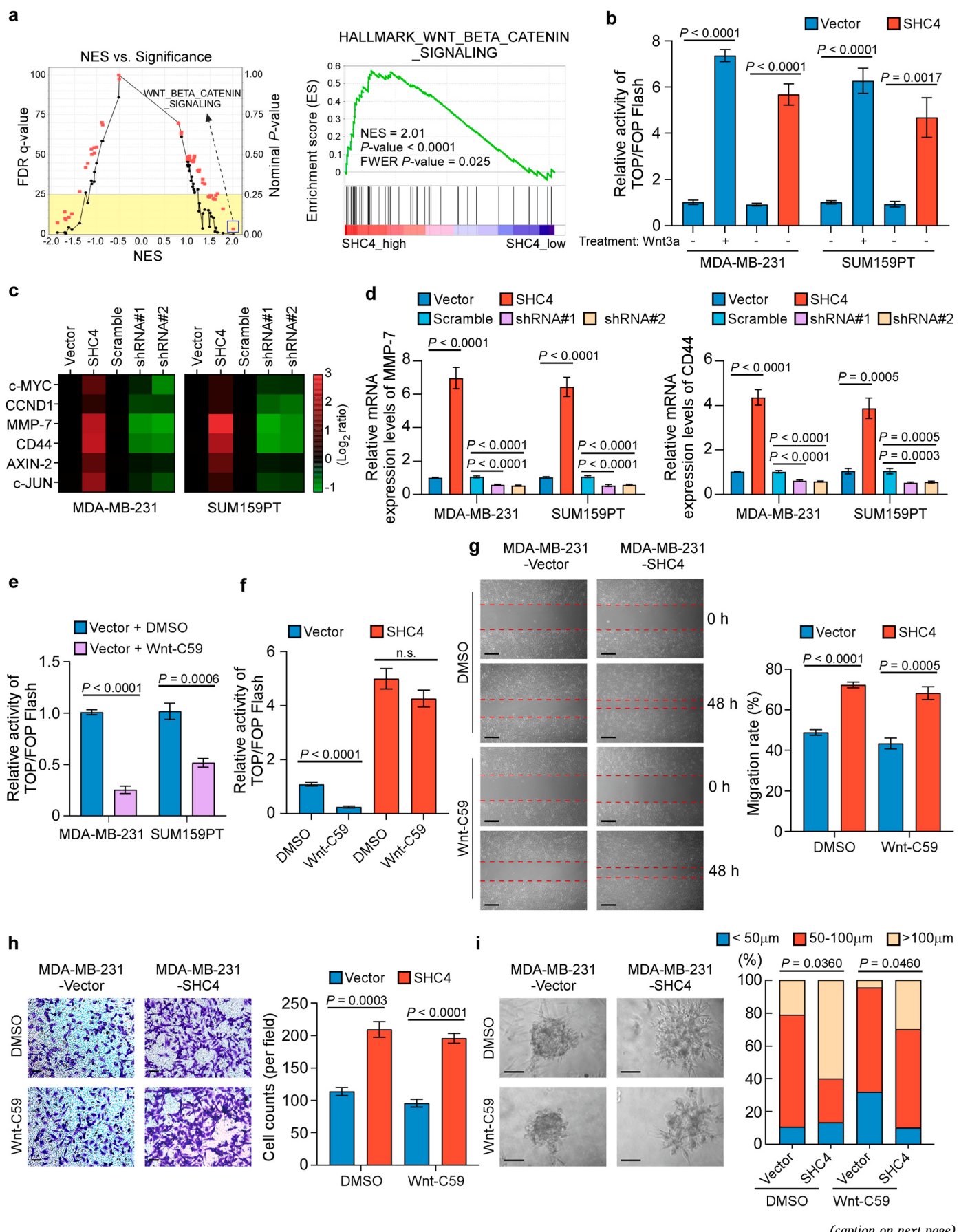
Given that  $\beta$ -catenin can be activated in a Wnt-independent manner, we explored the role of SHC4 in  $\beta$ -catenin signaling. SHC4-interacting proteins in TNBC cells were identified with SDS-PAGE, silver staining, and MS analysis, which identified Src kinase as a potent SHC4-interacting protein (Fig. 5a and b). The interacting protein network of SHC4 extracted from open-source prediction of the STRING functional interactions website (<https://string-db.org/>) also suggested that, with a combined STRING score of 0.868, Src kinase is a potential interaction candidate for both SHC4 and  $\beta$ -catenin (Fig. 5c). Immunofluorescence staining demonstrated that SHC4 and Src were highly co-localized in the cytoplasm (Fig. 5d). Furthermore, Co-IP using an anti-Src antibody revealed that Src bound to SHC4 in the MDA-MB-231 and SUM159PT cells. Reciprocally, the IP assays using anti-SHC4 antibodies demonstrated that the two proteins could form complexes endogenously (Fig. 5e, left and Supplementary Fig. 4a). Furthermore, Co-IP performed in 293T cells transfected with Flag-SHC4 and HA-Src confirmed that SHC4 also interacted with Src protein exogenously (Fig. 5e, right).

The phosphorylation of residues at different Src and  $\beta$ -catenin sites have specific functions. For example, Src-Y419 phosphorylation is an Src

kinase activation marker, while  $\beta$ -catenin-pY654 and -pS675 phosphorylation promote  $\beta$ -catenin detachment from the cell membrane into the cytoplasm and subsequent translocation to the nucleus. Next, we examined Src kinase and  $\beta$ -catenin phosphorylation levels in the MDA-MB-231 and SUM159PT cells with a series of commercial phosphorylated antibodies. The results demonstrated that overexpressing SHC4 increased Src-pY419,  $\beta$ -catenin-pY654, and  $\beta$ -catenin-pS675 levels, while silencing SHC4 exerted the opposite effect but did not influence Src and  $\beta$ -catenin protein expression (Fig. 5f and Supplementary Fig. 4b). The nuclear protein extraction assay indicated that SHC4 expression increased nuclear translocation of  $\beta$ -catenin while silencing SHC4 abrogated it (Fig. 5g). Notably, both the Src kinase inhibitor SKI-606 and mutant Src (Y419A) abrogated SHC4-induced Src phosphorylation and  $\beta$ -catenin activation in the TNBC cells (Fig. 5h and Supplementary Figs. 4c and 4d). These results suggested that  $\beta$ -catenin activation induced by SHC4 was achieved by promoting Src kinase Y419 phosphorylation.

### 3.6. SHC4 PxPPxPxxxPxxP is the key sequence for activating Src kinase

The identification of specific binding sites of Src and SHC4 is expected to provide strategies for developing inhibitors. We investigated the details of the interactions between SHC4 and Src, where truncated forms of SHC4 and Src were expressed and underwent IP assays. Only Src truncations with the SH3 domain could bind to SHC4, which suggested that this domain was responsible for its interaction with SHC4 (Fig. 6a). Conversely, the CH2 domain was essential for SHC4 interaction with Src (Fig. 6b). The mechanisms of Src kinase activation include destabilization of the intramolecular interactions involving the SH3 and SH2 domains by phosphatases, kinases or adaptor proteins with PxxP and/or phosphotyrosine-containing motifs that shift the conformational equilibrium to an “open” active state [18]. It was also suggested that the PxxP-containing proteins WASp [19], the PI3K p85 subunit [20], and androgen receptor (AR) [21] can bind or activate Src kinase. Interestingly, the SHC4 peptide sequence analysis determined that the Src SH3 domain recognized the three PxxP motif-containing segments of CH2. IP assays using anti-Src antibody in MDA-MB-231 cells with or without SHC4 overexpression demonstrated that overexpressing SHC4 markedly increased the endogenous interactions between Src and SHC4 (Fig. 6c). Then, we designed three mutants to interfere with the possible binding sites, where the prolines (P) in each of the three PxxP-containing segments were replaced with alanines (A). Notably, SHC4 mutant 1, but not mutant 2 or 3 abrogated the interaction between SHC4 and Src, which indicated that the mutant 1 PxPPxPxxxPxxP sequence was crucial for Src SH3 domain recognition (Fig. 6d). Furthermore, TOP/FOP-Flash activity assays indicated that reconstitution of wild-type SHC4 and SHC4 mutants with the PxPPxPxxxPxxP sequence (SHC4-mut2 and SHC4-mut3) activated  $\beta$ -catenin signaling (Supplementary Fig. 5a). Reconstitution of wild-type SHC4 and SHC4 mutants with the PxPPxPxxxPxxP sequence facilitated Src kinase activation and the expression of downstream genes, and promoted  $\beta$ -catenin translocation to the nucleus and E-cadherin degradation (Fig. 6e and f). These findings indicated that the PxPPxPxxxPxxP sequence was necessary for the complete function of SHC4 in binding and activating Src kinase.



(caption on next page)

**Fig. 4. SHC4 activates  $\beta$ -catenin in a Wnt-independent manner.** (a) TCGA dataset GSEA demonstrated significant enrichment of a  $\beta$ -catenin-upregulated gene signature in SHC4-high samples. NES, normalized enrichment score. (b) Normalized luciferase activity of specific TOP-Flash over non-specific FOP-Flash relative RLU in vector and SHC4-overexpressing cells treated with Wnt3a or PBS. (c) Heat map of relative mRNA expression of  $\beta$ -catenin downstream target genes in MDA-MB-231 and SUM159PT cells. (d) RT-PCR examination of the relative expression levels of two typical  $\beta$ -catenin downstream genes: *MMP7* (left) and *CD44* (right). (e) TOP/FOP-Flash assay of dimethyl sulfoxide (DMSO)- or Wnt-C59-treated MDA-MB-231 and SUM159PT cells. (f) TOP/FOP-Flash assay of DMSO- or Wnt-C59-treated vector or SHC4-expressing MDA-MB-231 cells. (g) Representative images (left) and quantification (right) of wound healing assay of DMSO- or Wnt-C59-treated vector or SHC4-overexpressing MDA-MB-231 cells. (h) Representative images (left) and quantification (right) of transwell assay of DMSO- or Wnt-C59-treated vector or SHC4-overexpressing MDA-MB-231 cells. (i) Representative images (left) and quantification (right) of 3D spheroid culture assay of DMSO- or Wnt-C59-treated vector or SHC4-overexpression MDA-MB-231 cells. Scale bar: 50  $\mu$ m. Two-tailed Student's t-test and  $\chi^2$  test were used. Data represent the means  $\pm$  S.D. of three independent experiments.

### 3.7. Deletion of the PxPPxPxxxPxxP sequence inhibits TNBC progression *in vitro* and *in vivo*

We established SHC4-wild-type (SHC4-wt) and SHC4 mutant 1 (SHC4-mut1) in human and mouse TNBC cells. As expected, transduction with SHC4-mut1 impaired cell anchorage-independent TNBC cell growth, migration (*Supplementary Figs. 6a and 6b*), and invasion (*Fig. 7a* and b). Next, 4T1-luci cells stably overexpressing SHC4-wt or SHC4-mut1 were established, and were orthotopically injected into the mammary fat pads of mice. Expressing SHC4-mut1 decreased the lung metastatic burden (*Fig. 7c* and d). Furthermore, the phosphorylation of Src and  $\beta$ -catenin and the typical  $\beta$ -catenin downstream proteins MMP-7 and CD44 both decreased, but E-cadherin was increased in the orthotopic 4T1-luci-SHC4-mut1 tumor (*Fig. 7e* and f). Moreover, the lung colonization models yielded similar results (*Fig. 7g* and h). These findings suggested that the PxPPxPxxxPxxP sequence was necessary for SHC4 in binding and activating Src kinase.

### 3.8. Clinical relevance of SHC4-induced Src kinase and $\beta$ -catenin activation in TNBC

Finally, we evaluated the clinical relevance and significance of SHC4/Src (pY419)/ $\beta$ -catenin axis in TNBC. Significantly, IHC staining and subsequent correlation analysis revealed that SHC4 positively correlated with Src (pY419) and nuclear  $\beta$ -catenin in 112 TNBC patient specimens (*Fig. 8a* and b). Importantly, Kaplan-Meier survival curves and log-rank tests revealed that TNBC patients with combined high SHC4 expression, high Src (pY419) expression and positive nuclear  $\beta$ -catenin expression, suffered poorest OS and DMFS (*Fig. 8c*). Furthermore, the combined three factors, advanced T stage and advanced N stage were identified as independent prognostic factors for five-year DMFS in TNBC by multivariate regression analysis (*Supplementary Table 3*). Taken together, our findings suggested that SHC4 activated  $\beta$ -catenin by promoting Src kinase autophosphorylation to enhance TNBC metastasis and poor clinical outcomes.

## 4. Discussion

Distant metastasis remains the primary challenge in TNBC treatment, and results in poor prognosis. Patients with TNBC present with a higher incidence of distant disease recurrence within 3 years after diagnosis, and with a high frequency of visceral metastases [1,22]. Once metastasis occurs, TNBC is incurable, with a median OS that averages only 10–13 months [23]. In the present study, SHC4 was identified as a vital protein in TNBC progression. Our results revealed that SHC4 was specifically upregulated in TNBC, which contributed to its highly metastatic activity and poor clinical outcomes. Furthermore, overexpressing SHC4 promoted TNBC cell invasion *in vitro* and metastasis *in vivo*. Subsequently, we determined that overexpressed SHC4 interacted with and promoted Src autophosphorylated activation, which resulted in  $\beta$ -catenin phosphorylation and nuclear translocation. Finally, we demonstrated that the SHC4 PxPPxPxxxPxxP sequence was necessary for activating Src kinase and that deleting the sequence inhibited TNBC progression *in vitro* and *in vivo*. Therefore, our results revealed a prognostic marker and future therapeutic target in TNBC.

$\beta$ -catenin is also known as an Armadillo protein that regulates gene expression following Wnt pathway activation. However, it is important to note that while the canonical Wnt signaling pathway activates  $\beta$ -catenin, it can also be activated by other signaling pathways [24]. Generally,  $\beta$ -catenin signaling enrichment is evident in TNBC, and patients with dysregulated  $\beta$ -catenin signaling are more likely to develop lung and brain secondary metastases [9,25]. However, comprehensive genomic analysis revealed that activating mutations of certain Wnt- $\beta$ -catenin pathway components such as APC and  $\beta$ -catenin were rarely observed in breast cancer [26], which indicated that alternative mechanisms, probably Wnt-independent, exist to activate  $\beta$ -catenin. Here, we first discovered that SHC4 activated  $\beta$ -catenin signaling to promote cancer invasion and metastasis in a Wnt-independent manner in TNBC. Our finding demonstrated that SHC4 activated  $\beta$ -catenin signaling without added Wnt ligands. Wnt-C59 inhibited Wnt3A-mediated activation of Wnt signaling activity in MDA-MB-231-vector cells, although it could not affect their migration or invasion. However, Wnt-C59 did not inhibit SHC4-mediated  $\beta$ -catenin activation or cell migration and invasion. Notably, Smits et al. proved that Y654-phosphorylated  $\beta$ -catenin demonstrates increased phosphorylation at S675 by protein kinase A (PKA) and increases tumor initiation by enhancing Wnt signaling in intestinal tumor [27]. In agreement with these previous researches, we determined that SHC4 promoted Src autophosphorylation activation, which resulted in  $\beta$ -catenin phosphorylation at Y654 and affinity reduction for E-cadherin. Subsequently, the accumulated cytoplasmic  $\beta$ -catenin was further phosphorylated at S675, which promoted  $\beta$ -catenin translocation into the nucleus to activate the transcription and expression of the invasion and metastasis-related genes *MMP7* and *CD44* (*Fig. 8d*).

As mentioned above, Src kinase autophosphorylation is important in Wnt-independent  $\beta$ -catenin signaling pathway activation. Src kinase is a prototypical modular signaling protein whose conserved domain organization includes a myristoylated N-terminal segment, followed by the SH3, SH2, and tyrosine kinase domains, and a short C-terminal tail [28]. The apparatus controlling Src activity contains three components termed the latch, the clamp, and the switch [29]. The SH2 domain binds to pY530 in the C-terminal tail to form the latch, which stabilizes SH2 domain attachment to the large kinase lobe. The linker between the SH2 and kinase domains is part of a motif that binds to the SH3 domain and attaches the SH3 domain to the small kinase lobe. The clamp is an assembly of the SH2 and SH3 domains behind the kinase domain and locks the kinase in an inactive conformation. Generally, when pY530 is dephosphorylated by phosphatases and displaced from the SH2-binding pocket (unlatching), Src kinase can then be autophosphorylated at Y419 by a partner Src molecule (switching) after the binding of competing ligands to their SH2 and/or SH3 domains (unclamping) [18,30]. Nonetheless, Moarefi et al. reported that Nef, an HIV-1 accessory factor that lacks catalytic activity, engages the Hck kinase SH3 domain, displacing it from the SH2-kinase linker and leading to kinase activation, while the SH2 domain remains engaged with the C-terminal tail [31]. Mutagenesis established that one determinant of Nef-SH3 interaction is the consensus proline-rich motif PxxP in Nef [32]. Intriguingly, we found three sequences containing PxxP motifs on the SHC4 CH2 domain, which suggested that it might be a potential Src-SH3 ligand. We determined that the PxPPxPxxxPxxP sequence on the SHC4 CH2 domain is

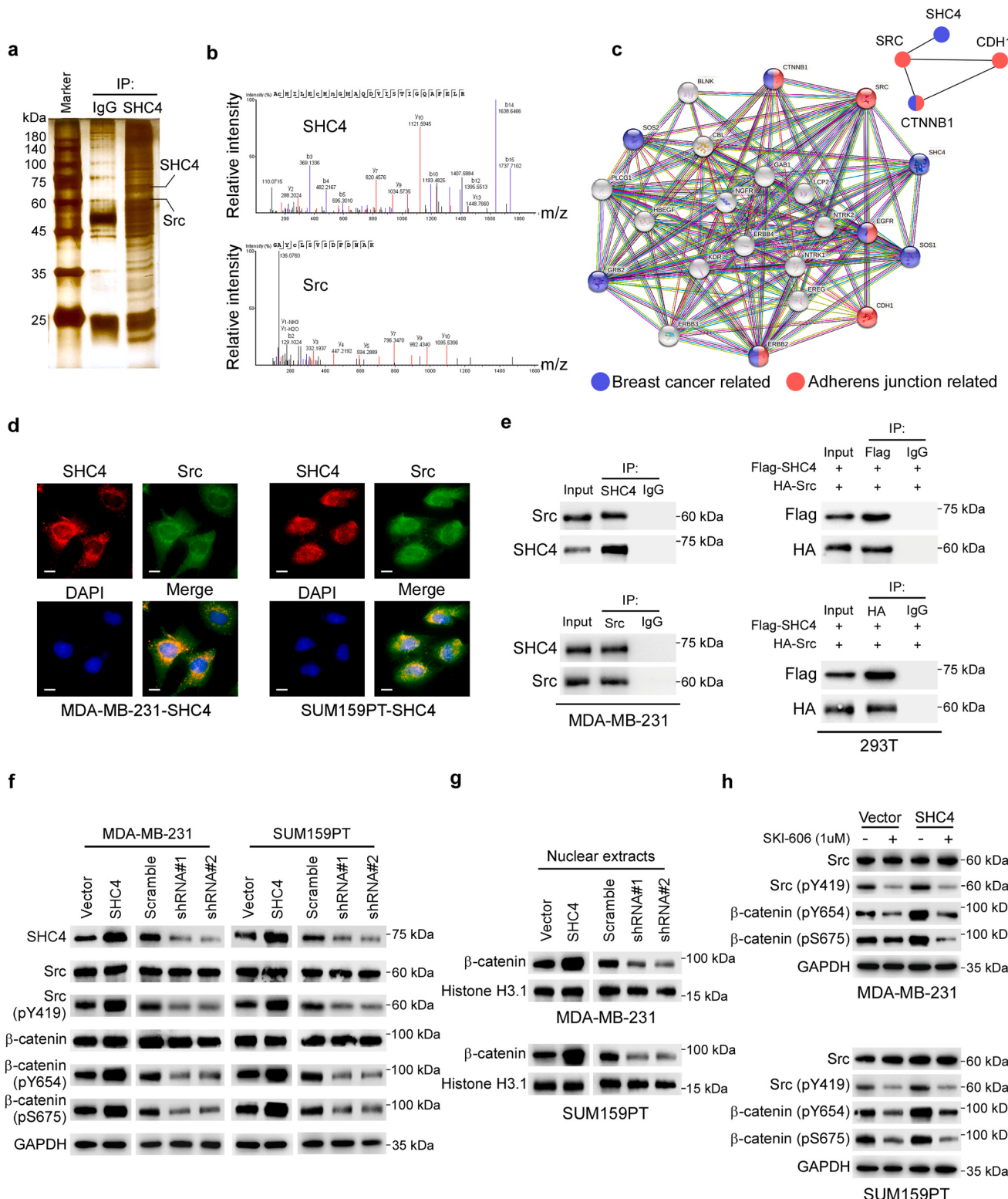
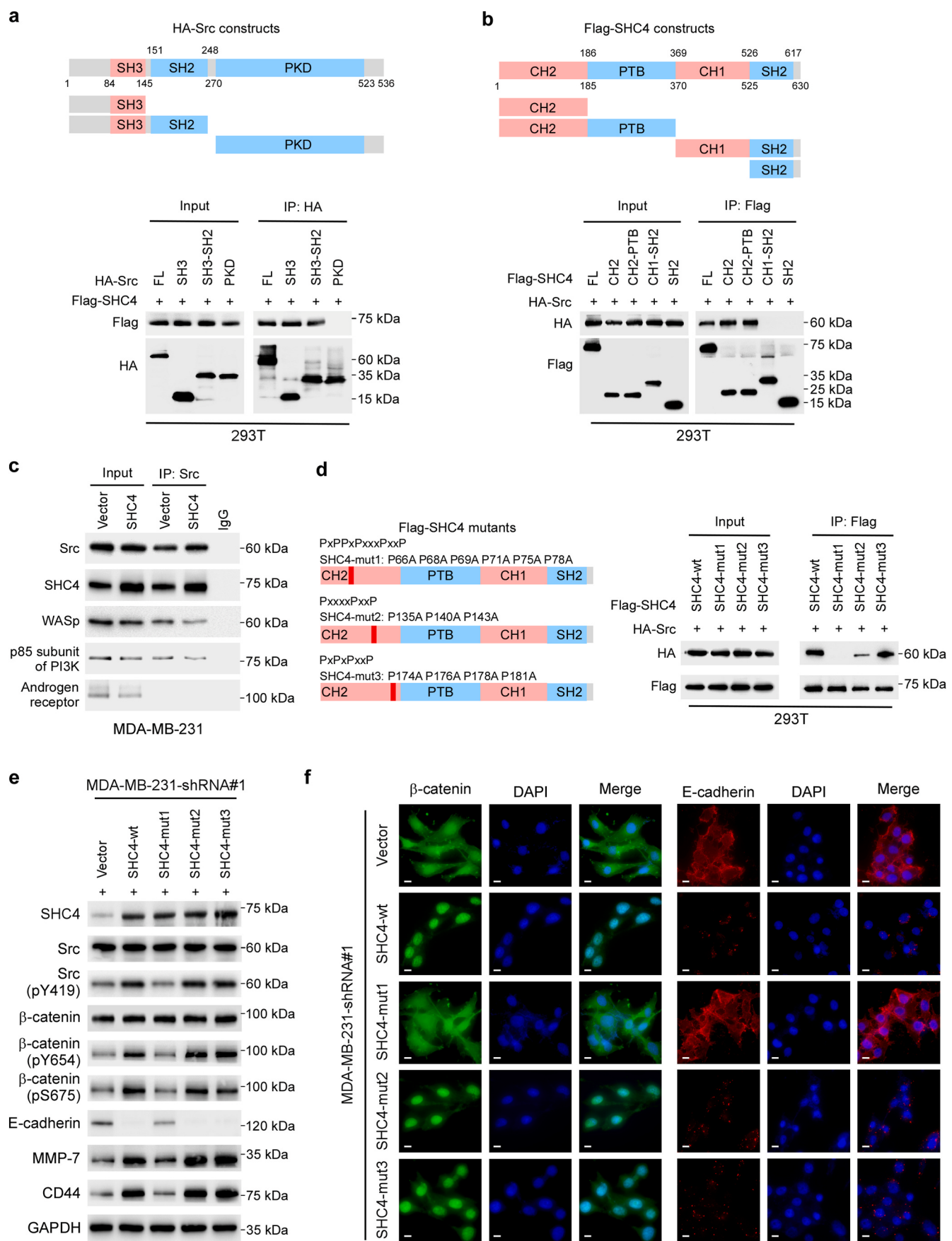


**Fig. 5. SHC4 binds and activates Src kinase by promoting its autophosphorylation at Y419.** (a) IP of the SHC4-interacting protein Src that involved SDS-PAGE, silver staining, and MS identification. (b) Representative MS plots and sequences of peptides from SHC4 (top) and Src (bottom). (c) Network image of predicted SHC4 binding partners accessed using the STRING database, where genes are represented as nodes. (d) Immunofluorescence staining of SHC4 and Src to examine their colonization in MDA-MB-231-SHC4 and SUM159PT-SHC4 cells. Scale bar: 10 μm. (e) IP assays determined the interaction between endogenous SHC4 and Src in MDA-MB-231 cells (left). IP assays were performed on 293T cells transfected with Flag-SHC4 and HA-Src (right). (f) Western blotting assays of SHC4, Src, Src-pY419, β-catenin, β-catenin-pY654, and β-catenin-pS675 in the MDA-MB-231 and SUM159PT cells. The loading control was GAPDH. (g) Nuclear fractions were extracted and underwent examination for β-catenin. The nuclear loading control was histone H3.1. (h) Src and Src-pY419 expression levels in control and SHC4-overexpressing MDA-MB-231 and SUM159PT cells treated with or without SKI-606 or 0.01 % DMSO for 3 h. The loading control was GAPDH.



(caption on next page)

**Fig. 6. SHC4 PxPPxPxxxPxxP is the key sequence for activating Src kinase.** (a) Schematic of HA-Src truncations (top). 293T cells were transfected with HA-Src truncations and Flag-SHC4, followed by IP assays with HA-beads to examine their interaction with SHC4 (bottom). (b) Schematic illustration of SHC4 truncated constructs (top). 293T cells were transfected with indicated Flag-tagged SHC4 truncations and HA-Src, followed by IP assays with Flag-beads to examine their interaction with Src (bottom). (c) IP assays of Src in MDA-MB-231 cells with or without SHC4 overexpression. (d) Schematic illustration of SHC4 mutants (left). 293T cells were transfected with indicated Flag-tagged SHC4 mutants and HA-Src, followed by IP assays with Flag-beads to examine their interaction with Src (right). (e) Western blotting assays of SHC4, Src,  $\beta$ -catenin, and related downstream proteins in SHC4-silenced MDA-MB-231 cells with restoration of SHC4 wild-type and mutants. The loading control was GAPDH. (f) Immunofluorescence staining of  $\beta$ -catenin and E-cadherin expression in SHC4-silenced MDA-MB-231 cells with restoration of SHC4 wild-type and mutants. Scale bar: 10  $\mu$ m.

critical for binding the SH3 domain and activating Src kinase. While SHC4-mut2 partially abrogated the interaction with Src, but this interference did not affect the activity of Src kinase. And SHC4-mut3 neither interfered with the interaction with Src nor affected the activity of Src kinase. We speculate that these differences in interaction and activation may be due to potential differences in the poly-L-proline type II (PPII) helix structure, which results in different affinities with the Src-SH3 domain [33,34]. And further analysis such as X-ray and Nuclear Magnetic Resonance (NMR) Spectroscopy are needed to confirm this hypothesis. Notably, Migliaccio's group synthesized a 10-amino acid peptide that simulated only the 377–386 sequence of human AR (Ac-PPP<sup>PH</sup>HARIK-NH<sub>2</sub>, S1 peptide). This peptide (1.0 M) inhibited the G1-to-S transition of androgen-stimulated prostate and mammary cancer cells *in vitro* and was also effective in a xenograft nude mouse model over 5-week intraperitoneally administered treatment [21]. Therefore, our results might have implications for future strategies for designing Src kinase inhibitors and provide a theoretical basis for Src kinase inhibitor treatment in patients with TNBC with SHC4 overexpression. Moreover, the SHC adaptor protein family lacks intrinsic enzymatic activity and the family members typically act as recruiting and conducting signaling molecules in signaling pathways. However, Wills et al. observed that SHC4 unexpectedly enhanced EGFR autophosphorylation even in the absence of external stimuli but failed to influence major signaling nodes through EGFR [35]. In the present study, we determined that SHC4 bound to the Src kinase SH3 domain via the PxPPxPxxxPxxP sequence on the CH2 domain, promoted Src autophosphorylation activation, and activated  $\beta$ -catenin signaling. This function is rare among SHC proteins and signaling scaffolds, which suggested that SHC4 might play a new role in TNBC signaling pathways.

The metastatic breast cancer process is complex, dynamic, and multi-step, and includes metastatic cells that undergo detachment, migration, invasion, and adhesion. These metastatic steps are inter-related and affected by multiple biochemical events and parameters such as abnormal activation of certain signaling pathways and epithelial-mesenchymal transition (EMT) [36,37]. However, a key EMT feature is the loss of cellular junctions such as the adherens junctions (AJs). AJs consist of E-cadherin-based cellular junctions attached to the actin cytoskeleton by catenin proteins, which are critical in epithelial cell integrity, tissue formation, and tumor suppression [38]. Cadherin-catenin complex structural and functional integrity is regulated by phosphorylation [39,40]. In the present study, SHC4-activated Src phosphorylated  $\beta$ -catenin at Y654 to induce its shedding from the AJ complex, and the loss of this interaction led to E-cadherin degradation and AJ disassembly *in vitro* and *vivo*. However, we determined that SHC4-overexpressing TNBC cells had elevated MMP7 and CD44 transcriptional activation and expression and increased E-cadherin degradation. Furthermore, increased transcriptional activity of MMPs other than MMP-7, such as MMP-2, MMP-9, and MMP-14 was also observed (Supplementary Figs. 7a and 7b). The synergistic effect of SHC4 and Src on invasion was observed in a TNBC cell-derived 3D spheroid invasion assay. We speculated that SHC4-induced Src activation and  $\beta$ -catenin activation by Src promote TNBC metastasis by regulating EMT and invadopodia formation. On the one hand, MMPs are the most functionally significant proteases responsible for cleaving cell-cell adhesion molecules and facilitating invadopodia activity in cancer cells. MMP-14 is not only an invasion-promoting component, but is also a master regulator of invadopodia development and maturation [41], while

MMP-2, -7, and -9 are secreted around invadopodia and promote local extracellular matrix (ECM) degradation [42]. However, we performed Gelatin zymography experiments and the results showed that both SHC4 overexpression and reconstitution of wild-type SHC4 and SHC4-mut2/3 (which contain PxPPxPxxxPxxP sequence) in SHC4-depleted background slightly increased, while knockdown SHC4 inhibited enzymatic activity of MMP-2 and MMP-9, mildly (Supplementary Fig. 7c). Because the expression and activation of MMP2 and MMP9 are regulated by various factors, including natural inhibitors TIMP-1/2, growth factors, and extracellular matrix degradation products [43]; therefore, further investigation is needed to explore the relationship between SHC4 and the formation of invasive pseudopods, as well as the activation of MMPs. On the other hand, a non-kinase cell surface transmembrane glycoprotein, CD44 binds directly to MMP-14 and mediates its proteolytic cleavage, thereby stimulating migration [44]. The CD44s splice isoform interacted with phosphorylated cortactin-activated invadopodia, enabling breast tumor cells to degrade ECM and metastasize to distant organs such as the lungs. Depleting CD44s eliminated invadopodia activity, prevented ECM degradation, and reduced tumor cell invasion and metastasis [45]. Additionally, increased Src activity promoted invadopodia bud formation [46] and shifted the cellular adhesome towards invadosome formation [47]. Notably, a recent report indicated that expression of SHC4 and the receptor tyrosine kinase Tie2 increased invasion and invadopodia formation and matrix degradation in U87 glioma cells [13]. Although we did not observe SHC4 involvement in invadopodia formation and regulation, our results highlighted a molecular mechanism to support the potential involvement of SHC4 in poor outcomes in TNBC.

## 5. Conclusions

We have determined that the PxPPxPxxxPxxP sequence on the SHC4 CH2 domain is critical for binding and activating the Src SH3 domain, which then promotes the Wnt-independent  $\beta$ -catenin signaling pathway and the transcription of invasion-related genes. Understanding the role of SHC4 in TNBC aggression and metastasis can increase knowledge of the biological basis of TNBC malignant progression and underscores its potential as a prognostic marker and future therapeutic target.

## CRediT authorship contribution statement

**Wenjing Zhong:** Writing – original draft, Methodology, Investigation, Formal analysis, Data curation, Conceptualization. **Yunting Jian:** Methodology, Investigation, Formal analysis, Data curation, Conceptualization. **Chao Zhang:** Methodology, Investigation, Formal analysis, Data curation, Conceptualization. **Yue Li:** Writing – review & editing. **Zhongyu Yuan:** Data curation, Formal analysis, Resources. **Zhenchong Xiong:** Formal analysis, Data curation. **Weiling Huang:** Formal analysis, Data curation. **Ying Ouyang:** Formal analysis, Data curation. **Xiangfu Chen:** Formal analysis, Data curation. **Libing Song:** Supervision, Project administration, Funding acquisition, Conceptualization. **Pian Liu:** Supervision, Project administration, Funding acquisition, Conceptualization. **Xi Wang:** Supervision, Project administration, Funding acquisition, Conceptualization.

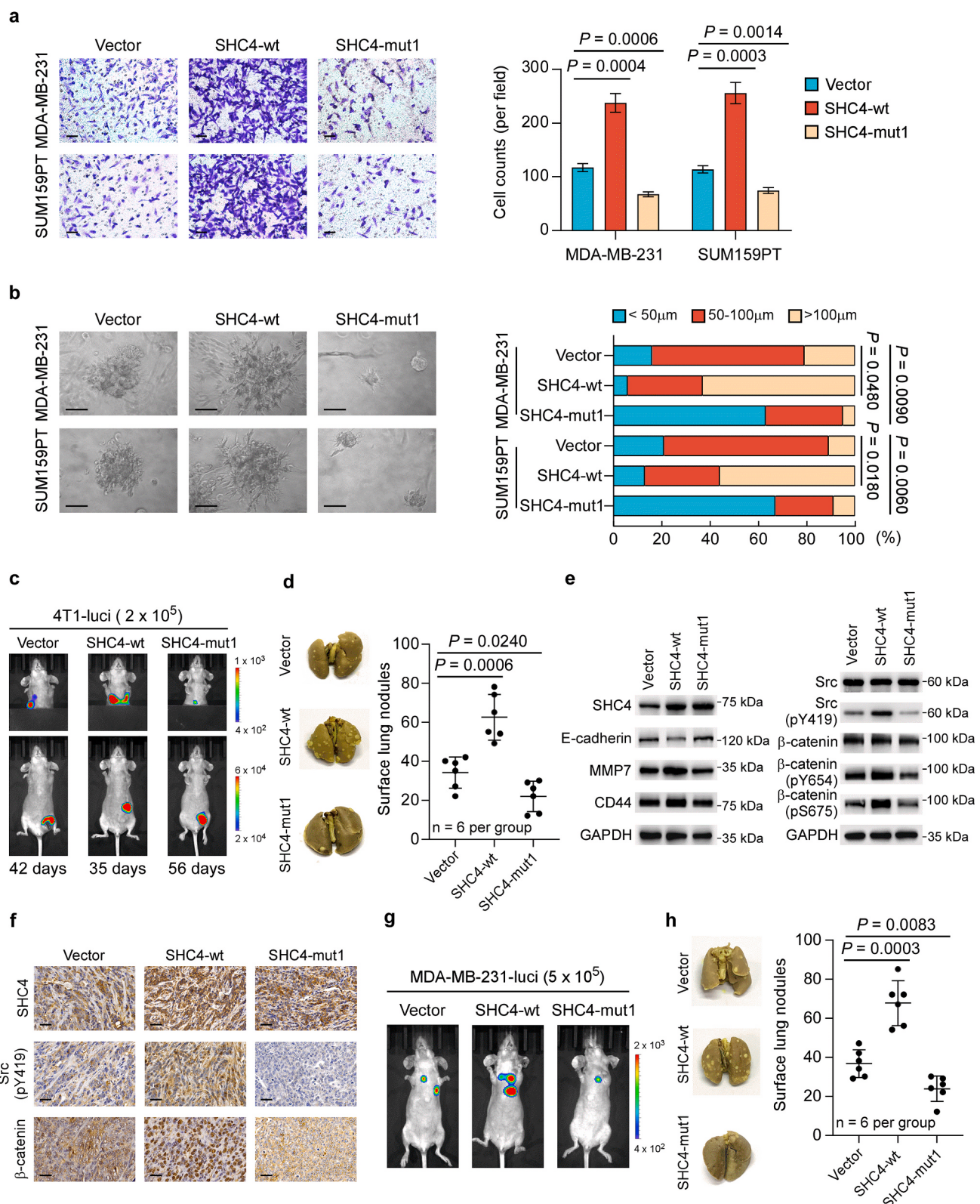


**Fig. 7. Deletion of the PxPPPxxPxxxPxxP sequence inhibits TNBC progression *in vitro* and *in vivo*.** (a, b) Representative images (left) and quantification (right) of transwell migration assay (a) and 3D spheroid culture assay (b). (c) Orthotopic xenograft model and spontaneous metastasis model: 4T1-luci cells stably transfected with control, SHC4-wt, or SHC4-mut1 were injected into the mammary fat pads of nude mice. The lung metastasis burden of each group was monitored weekly using BLI. (d) Representative bright-field imaging (left) and the number of visible surface lesions (right). Data are reported as the mean  $\pm$  S.D.. (e) Western blot analysis of SHC4 and related downstream protein in SHC4-overexpressing, SHC4-silenced, and control tumors. The loading control was GAPDH. (f) IHC staining of SHC4, pY419-Src, and β-catenin in 4T1-luci tumors. (g) Lung colonization model of SHC4-wt, SHC4-mut1, and control MDA-MB-231-luci cells. Representative BLI of lung metastasis is shown. (h) Representative bright-field imaging (left) and the number of visible surface lesions (right). Scale bar: 50 μm. Two-tailed Student's t-test and  $\chi^2$  test were used. Data represent the means  $\pm$  S.D. of three independent experiments.

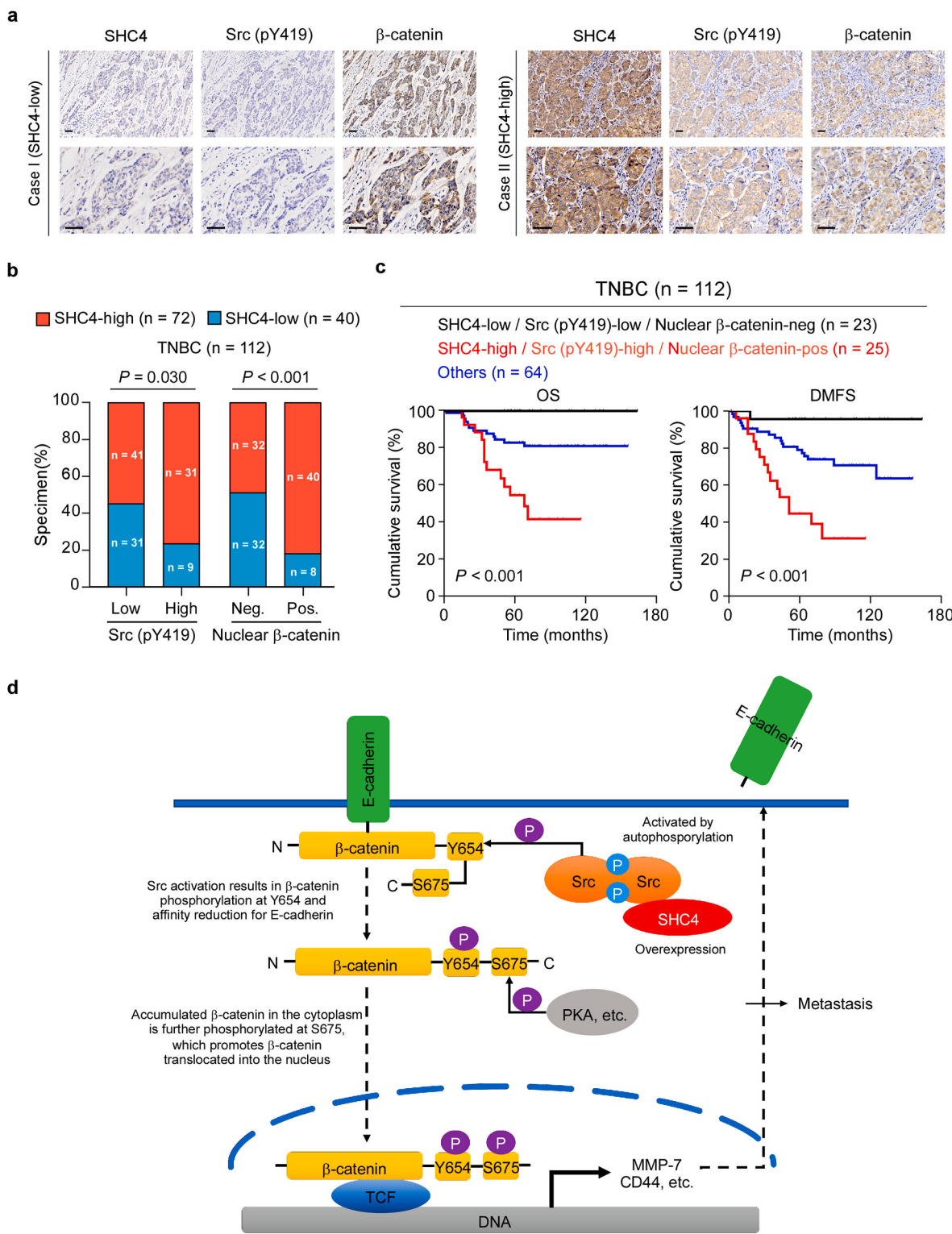


**Fig. 8. Clinical relevance of SHC4-induced β-catenin activation in TNBC and proposed model. (a)** Representative images of SHC4, Src (pY419), and nuclear β-catenin staining. Scale bar: 50 μm. **(b)** Distribution and correlation between SHC4 expression and Src (pY419) and nuclear β-catenin staining, via the  $\chi^2$  test. **(c)** OS (left) and DMFS (right) curves of 112 patients with TNBC stratified by SHC4-low/Src (pY419)-low/Nuclear β-catenin negative, SHC4-high/Src (pY419)-high/Nuclear β-catenin positive, and others (log-rank test). **(d)** Proposed model: SHC4 activates β-catenin by promoting Src kinase autophosphorylation to enhance TNBC metastasis.

#### Declaration of competing interest

The authors declare that they have no known competing financial interests or personal relationships that could have appeared to influence

the work reported in this paper.

## Acknowledgements

This work was supported by the National Key Research and Development Program of China (No. 2020YFA0509400), the National Natural Science Foundation of China (No. 81972459, 81772800, 82072945, 82202850, 82003052 and 82372947), the Natural Science Foundation of Guangdong Province (No. 2019A151011781, 2023A1515010375), and Science and Technology Projects in Guangzhou (No. SL2022A04J01247).

## Appendix A. Supplementary data

Supplementary data to this article can be found online at <https://doi.org/10.1016/j.canlet.2023.216516>.

## References

- [1] A. Ignatov, H. Eggemann, E. Burger, T. Ignatov, Patterns of breast cancer relapse in accordance to biological subtype, *J. Cancer Res. Clin. Oncol.* 144 (2018) 1347–1355.
- [2] F. Borri, A. Granaglia, Pathology of triple negative breast cancer, *Semin. Cancer Biol.* 72 (2021) 136–145.
- [3] A.C. L.N. Garrido-Castro, K. Polyak, Insights into molecular classifications of triple-negative breast cancer: improving patient selection for treatment, *Cancer Discov.* 9 (2) (2019) 176–198.
- [4] D.A.C. Bianchini G, L. Licata, L. Gianni, Treatment landscape of triple-negative breast cancer - expanded options, evolving needs, *Nat. Rev. Clin. Oncol.* 19 (2) (2022) 91–113.
- [5] S. M.S. Roura, J. Piedra, A. García de Herreros, M. Duñach, Regulation of E-cadherin/catenin association by tyrosine phosphorylation, *J. Biol. Chem.* 274 (51) (1999) 36734–36740, 17.
- [6] A. Danilkovich-Miagkova, A. Miagkov, A. Skeel, N. Nakagawa, B. Zbar, E. J. Leonard, Oncogenic mutants of RON and MET receptor tyrosine kinases cause activation of the  $\beta$ -catenin pathway, *Mol. Cell Biol.* 21 (2001) 5857–5868.
- [7] W.J. Nelson, R. Nusse, Convergence of Wnt, beta-catenin, and cadherin pathways, *Science* 303 (2004) 1483–1487.
- [8] A.I. Khrantsov, G.F. Khrantsova, M. Tretiakova, D. Huo, O.I. Olopade, K.H. Goss, Wnt/beta-catenin pathway activation is enriched in basal-like breast cancers and predicts poor outcome, *Am. J. Pathol.* 176 (2010) 2911–2920.
- [9] X. Xu, M. Zhang, F. Xu, S. Jiang, Wnt signaling in breast cancer: biological mechanisms, challenges and opportunities, *Mol. Cancer* 19 (2020) 165.
- [10] S.B.M. Ahmed, S.A. Prigent, Insights into the shc family of adaptor proteins, *J. Mol. Signal.* 12 (2017) 2.
- [11] R. Ks, Signaling via Shc family adapter proteins, *Oncogene* 20 (44) (2001) 6322–6330, 1.
- [12] E. Fagiani, G. Giardina, L. Luzi, M. Cesaroni, M. Quarto, M. Capra, G. Germano, M. Bono, M. Capillo, P. Pelicci, L. Lanfrancone, RaLP, a new member of the Src homology and collagen family, regulates cell migration and tumor growth of metastatic melanomas, *Cancer Res.* 67 (2007) 3064–3073.
- [13] M. Tilak, B. Alural, S.E. Wismer, M.I. Brasher, L.A. New, S.D. Sheridan, R.H. Perlis, M.G. Coppolino, J. Lalonde, N. Jones, Adaptor protein ShcD/SHC4 interacts with Tie2 receptor to synergistically promote glioma cell invasion, *Mol. Cancer Res.* 19 (2021) 757–770.
- [14] X. Zhang, H. Zhang, Z. Liao, J. Zhang, H. Liang, W. Wang, J. Yu, K. Dong, SHC4 promotes tumor proliferation and metastasis by activating STAT3 signaling in hepatocellular carcinoma, *Cancer Cell Int.* 22 (2022) 24.
- [15] A. Maind, S. Raut, Identifying condition specific key genes from basal-like breast cancer gene expression data, *Comput. Biol. Chem.* 78 (2019) 367–374.
- [16] K. Goto, M. Ishikawa, D. Aizawa, K. Muramatsu, M. Naka, T. Sugino, Nuclear  $\beta$ -catenin immunoexpression in scars, *J. Cutan. Pathol.* 48 (2021) 18–23.
- [17] W.E. Kadowaki T, J. Klingensmith, K. Zachary, N. Perrimon, The segment polarity gene *porcupine* encodes a putative multitransmembrane protein involved in Wingless processing, *Genes Dev.* 10 (24) (1996) 3116–3128. Dec 15.
- [18] M.A. Ortiz, T. Mikhailova, X. Li, B.A. Porter, A. Bah, L. Kotula, Src family kinases, adaptor proteins and the actin cytoskeleton in epithelial-to-mesenchymal transition, *Cell Commun. Signal.* 19 (2021) 67.
- [19] Y. Shi, B. Dong, H. Miliotis, J. Liu, A.S. Alberts, J. Zhang, K.A. Siminovitch, Src kinase Hck association with the WASp and mDia1 cytoskeletal regulators promotes chemoattractant-induced Hck membrane targeting and activation in neutrophils, *Biochem. Cell. Biol.* 87 (2009) 207–216.
- [20] J.J. Song, J.H. Kim, B.K. Sun, M.A. Alcalá Jr., D.L. Bartlett, Y.J. Lee, c-Cbl acts as a mediator of Src-induced activation of the PI3K-Akt signal transduction pathway during TRAIL treatment, *Cell. Signal.* 22 (2010) 377–385.
- [21] A. Migliaccio, L. Varricchio, A. De Falco, G. Castoria, C. Arra, H. Yamaguchi, A. Ciociola, M. Lombardi, R. Di Stasio, A. Barbieri, A. Baldi, M.V. Barone, E. Appella, F. Auricchio, Inhibition of the SH3 domain-mediated binding of Src to the androgen receptor and its effect on tumor growth, *Oncogene* 26 (2007) 6619–6629.
- [22] K. Kast, T. Link, K. Friedrich, A. Petzold, A. Niedostatek, O. Schoffer, C. Werner, S. J. Klug, A. Werner, A. Gatzweiler, B. Richter, G. Baretton, P. Wimberger, Impact of breast cancer subtypes and patterns of metastasis on outcome, *Breast Cancer Res. Treat.* 150 (2015) 621–629.
- [23] M.K. Malhotra, L.A. Emens, The evolving management of metastatic triple negative breast cancer, *Semin. Oncol.* 47 (2020) 229–237.
- [24] Z. Aktary, J.U. Bertrand, L. Larue, The WNT-less wonder: WNT-independent  $\beta$ -catenin signaling, *Pigment Cell & Melanoma Research* 29 (2016) 524–540.
- [25] B.B. Dey N, C.S. Moreno, M. Ordanic-Kodani, Z. Chen, G. Oprea-Ilie, W. Tang, C. Catzavelos, K.F. Kerstann, G.W. Sledge Jr., M. Abramovitz, M. Bouzyk, P. De, B. R. Leyland-Jones, Wnt signaling in triple negative breast cancer is associated with metastasis, *BMC Cancer* 13 (2013) 537. Nov 10.
- [26] F.C. Geyer, M. Lacroix-Triki, K. Savage, M. Arnedos, M.B. Lambros, A. MacKay, R. Natrajan, J.S. Reis-Filho, beta-Catenin pathway activation in breast cancer is associated with triple-negative phenotype but not with CTNNB1 mutation, *Mod. Pathol.* 24 (2011) 209–231.
- [27] W. van Veelen, N.H. Le, W. Helvensteijn, L. Blonden, M. Theeuwes, E.R. Bakker, P. F. Franken, L. van Gurp, F. Meijlink, M.A. van der Valk, E.J. Kuipers, R. Fodde, R. Smits, beta-catenin tyrosine 654 phosphorylation increases Wnt signalling and intestinal tumorigenesis, *Gut* 60 (2011) 1204–1212.
- [28] B.J. Thomas Sm, Cellular functions regulated by Src family kinases, *Annu. Rev. Cell Dev. Biol.* 13 (1997) 513–609.
- [29] H. Sc, Variation on an src-like theme, *Cell* 112 (6) (2003) 737–740, 21.
- [30] R. Roskoski, Src protein-tyrosine kinase structure, mechanism, and small molecule inhibitors, *Pharmacol. Res.* 94 (2015) 9–25.
- [31] L.-B.M. Moarefi I, F. Sicheri, M. Huse, C.H. Lee, J. Kuriyan, W.T. Miller, Activation of the Src-family tyrosine kinase Hck by SH3 domain displacement, *Nature* 385 (6617) (1997) 650–653. Feb 13.
- [32] C.G. Saksela K, Baltimore D , Proline-rich (PxxP) motifs in HIV-1 Nef bind to SH3 domains of a subset of Src kinases and are required for the enhanced growth of Nef + viruses but not for down-regulation of CD4, *EMBO J.* 14 (3) (1995) 484–491. Feb 1.
- [33] A.A. Adzhubei, M.J.E. Sternberg, A.A. Makarov, Polyproline-II helix in proteins: structure and function, *J. Mol. Biol.* 425 (2013) 2100–2132.
- [34] J.J. Alvarado, L. Bettis, J.A. Morocco, T.E. Smithgall, J.I. Yeh, Crystal structure of the Src family kinase Hck SH3-SH2 linker regulatory region supports an SH3-dominant activation mechanism, *J. Biol. Chem.* 285 (2010) 35455–35461.
- [35] M.K.B. Wills, J. Tong, S.L. Tremblay, M.F. Moran, N. Jones, J. Chernoff, The ShcD signaling adaptor facilitates ligand-independent phosphorylation of the EGF receptor, *Mol. Biol. Cell* 25 (2014) 739–752.
- [36] X. Guan, Cancer metastases: challenges and opportunities, *Acta Pharm. Sin. B* 5 (2015) 402–418.
- [37] S. Al-Mahmood, J. Sapiezynski, O.B. Garbuzenko, T. Minko, Metastatic and triple-negative breast cancer: challenges and treatment options, *Drug Deliv Transl Res* 8 (2018) 1483–1507.
- [38] F. van Roy, G. Berx, The cell-cell adhesion molecule E-cadherin, *Cell. Mol. Life Sci.* 65 (2008) 3756–3788.
- [39] J. Lilien, J. Balsamo, C. Arregui, G. Xu, Turn-off, drop-out: functional state switching of cadherins, *Dev. Dynam.* 224 (2002) 18–29.
- [40] J. Piedra, S. Miravet, J. Castano, H.G. Palmer, N. Heisterkamp, A. Garcia de Herreros, M. Dunach, p120 Catenin-associated Fer and Fyn tyrosine kinases regulate beta-catenin Tyr-142 phosphorylation and beta-catenin-alpha-catenin Interaction, *Mol. Cell Biol.* 23 (2003) 2287–2297.
- [41] S. Niland, A.X. Riscanevo, J.A. Eble, Matrix metalloproteinases shape the tumor microenvironment in cancer progression, *Int. J. Mol. Sci.* 23 (2021).
- [42] O.Y. Revach, B. Geiger, The interplay between the proteolytic, invasive, and adhesive domains of invadopodia and their roles in cancer invasion, *Cell Adhes. Migrat.* 8 (2014) 215–225.
- [43] P.V. Kessenbrock K, Z. Werb, Matrix metalloproteinases: regulators of the tumor microenvironment, *Cell* 141 (1) (2010) 52–67. Apr 2.
- [44] T.T. Mori H, N. Koshikawa, M. Kajita, Y. Itoh, H. Sato, H. Tojo, I. Yana, M. Seiki, CD44 directs membrane-type 1 matrix metalloproteinase to lamellipodia by associating with its hemopexin-like domain, *EMBO J.* 21 (15) (2002) 3949–3959. Aug 1.
- [45] X.Y. Zhao P, Y. Wei, Q. Qiu, T.L. Chew, Y. Kang, C. Cheng, The CD44s splice isoform is a central mediator for invadopodia activity, *J. Cell Sci.* 129 (7) (2016) 1355–1365. Apr 1.
- [46] D.A. Murphy, S.A. Courtneidge, The 'ins' and 'outs' of podosomes and invadopodia: characteristics, formation and function, *Nat. Rev. Mol. Cell Biol.* 12 (2011) 413–426.
- [47] M. Oser, H. Yamaguchi, C.C. Mader, J.J. Bravo-Cordero, M. Arias, X. Chen, V. Desmarais, J. van Rheenen, A.J. Koleske, J. Condeelis, Cortactin regulates cofilin and N-WASp activities to control the stages of invadopodium assembly and maturation, *J. Cell Biol.* 186 (2009) 571–587.